Diphenylthienylamine-Based Star-Shaped Molecules for Electroluminescence Applications

Iuan-Yuan Wu, Jiann T. Lin,* Yu-Tai Tao,* E. Balasubramaniam, Yi Zhen Su, and Chung-Wen Ko

Institute of Chemistry, Academia Sinica, Taipei, Taiwan 115, Republic of China, Taiwan

Received January 23, 2001. Revised Manuscript Received May 30, 2001

Star-shaped compounds containing a triphenylamine as the central core and three diphenylthienylamines (NAr^1Ar^2(th): **3a**, $Ar^1 = Ar^2 =$ Ph; **3b**, $Ar^1 =$ Ph and $Ar^2 =$ 3-tolyl; **3c**, $Ar^1 =$ Ph and $Ar^2 =$ 1-naphthyl; **3d**, $NAr^1Ar^2 =$ carbazolyl) as the peripheral functional groups have been synthesized and characterized. These compounds exhibit four successive reversible one-electron redox processes except for **3d** in which only two one-electron reversible oxidation waves are observed. The compounds **3a**−**d** can be used as hole transport materials, and electroluminescent devices ITO/**3**/Alq [tris(8-quinolinolato)aluminum]/Mg:Ag emit green light characteristic of Alq. The device ITO/**3d**/BCP (bathocuproine)/Alq/Mg:Ag is blue emitting, in which **3d** is the luminophore.

Introduction

Organic light-emitting diodes (OLED) have recently received considerable attention because of their potential application to full-color flat-panel displays.[1] A number of low molecular weight organic materials and polymers have been studied for use as materials in organic electroluminescent (EL) devices. There have been extensive studies on layered organic EL devices with the aim of achieving high brightness and multicolor emission.[2] One major concern of organic EL materials is their durability, i.e., thermal and morphological stability. Amorphous materials may exhibit isotropic properties as well as homogeneous properties due to the absence of grain boundaries. Therefore, amorphous molecular materials with high glass transition temperature (T_g) are highly desirable. Furthermore, strain-driven failure[3] resulting from expansion of the charge transport layer in a thermally stressed OLED can be eased if materials of high T_g are used.

A very simple concept for the formation of amorphous glass is a nonplanar molecular structure because easy packing of molecules and hence ready crystallization can be avoided. Shirota have synthesized several novel families of organic π-electron starburst molecules which readily form amorphous glasses above room temperature because of an increase in the number of conformers together with nonplanar molecular structures.[4] Among these, derivatives of triarylamine, which form amorphous films on cooling from the melt or on casting appear to be interesting.[5]

Recently, we have successfully synthesized star-shaped compounds hexakis[(diarylamino)thienyl]benzene containing a hexathienylbenzene core with which was attached six peripheral diarylthienylamine substituents.[6] These compounds are promising hole transport materials because of their high thermal stability, high glass transition temperature, and low oxidation potential in comparison with commonly used hole transport materials, 1,4-bis[(1-naphthylphenyl)amino]-biphenyl (α-NPD; $T_g = 100$ °C) and 1,4-bis[(phenyl-*m*-tolyl)amino]biphenyl (TPD; $T_g = 60$ °C).[6] The lower oxidation potential of these compounds than those of α-NPD and TPD apparently are due to incorporation of an electron-rich thienyl ring[7] next to the nitrogen atom. Although Forrest found no clear correlation between the highest occupied molecular orbital (HOMO) energy and device quantum efficiency or turn-on voltage in devices fabricated from a series of triaryldiamines,[8] hole transport materials with different HOMO energies are potentially useful for multilayer OLED devices containing double hole transport layers.[9] Accordingly, we have set out to synthesize tris{[(diarylamino)thienyl]phenyl}-amine for potential hole transport materials. Herein, we report the synthesis, characterization, and fabrication of LED devices using these materials.

Experimental Section

All reactions and manipulations were carried out under N_2 with the use of a standard inert atmosphere and Schlenk

* Corresponding author. Fax: Int. code + (2)27831237. E-mail: jtlin@chem.sinica.edu.tw.

(1) Miyata, S., Nalwa, H. S., Eds. *Organic Electroluminescent Materials and Derivatives*; Gordon and Breach: New York, 1997.
(2) Chen, C. H.; Shi, J. *Coord. Chem. Rev.* **1998**, *171*, 161.
(3) Fenter, P.; Schreiber, F.; Bulovic, V.; Forrest, S. R. *Chem. Phys. Lett.* **1997**, *277*, 521.
(4) Shirota, Y. *J. Mater. Chem.* **2000**, *10*, 1.
(5) (a) Shirota, Y.; Kobata, T.; Noma, N. *Chem. Lett.* **1989**, 1145. (b) Higuchi, A.; Inada, H.; Kobata, T.; Shirota, Y. *Adv. Mater.* **1991**, *3*, 549. (c) Inada, H.; Shirota, Y. *J. Mater. Chem.* **1993**, *3*, 319. (d) Kuwabara, Y.; Ogawa, H.; Inada, H.; Noma, N.; Shirota, Y. *Adv. Mater.* **1994**, *6*, 677. (e) Katsuma, K.; Shirota, Y. *Adv. Mater.* **1998**, *10*, 223.
(6) Wu, I.-Y.; Lin, J. T.; Tao, Y.-T.; Balasubramaniam, E. *Adv. Mater.* **2000**, *12*, 668.
(7) Albert, I. D. L.; Marks, T. J.; Ratner, M. A. *J. Am. Chem. Soc.* **1997**, *119*, 6575.
(8) (a) O'Brien, D. F.; Burrows, P. E.; Forrest, S. R.; Koene, B. E.; Loy, D. E.; Thompson, M. E. *Adv. Mater.* **1998**, *10*, 1108. (b) Koene, B. E.; Loy, D. E.; Thompson, M. K. *Chem. Mater.* **1998**, *10*, 2235.
(9) (a) Shirota, Y.; Kuwabara, Y.; Okuda, D.; Okuda, R.; Ogawa, H.; Inada, H.; Wakimoto, T.; Nakada, H.; Yonemoto, Y.; Kawami, S.; Imai, K. *J. Lumin.* **1997**, *72*−*74*, 985. (b) Giebeler, C.; Antoniadis, H.; Bradley, D. D. C.; Shirota, Y. *J. Appl. Phys.* **1999**, *85*, 608.

10.1021/cm0100568 CCC: $20.00
Published on Web 06/29/2001

techniques. Solvents were dried by standard procedures. All column chromatographies were performed with the use of silica gel (230−400 mesh, Macherey-Nagel GmbH & Co.) as the stationary phase in a column 30 cm in length and 4.0 cm in diameter. The NMR spectra were recorded on Bruker AMX400 and AC300 spectrometers. Absorption and emission measurements were done using Cary 50 probe UV−visible and Hitachi F-4500 fluorescence spectrophotometers, respectively. Emission quantum yields were measured with reference to Coumarinn 1 dye [7-(diethylamino)-4-methylcoumarin] in ethyl acetate.[10] Cyclic voltammetry experiments were performed with a BAS-100 electrochemical analyzer. All measurements were carried out at room temperature with a conventional three-electrode configuration consisting of a platinum working, an auxiliary, and a nonaqueous $Ag/AgNO_3$ reference electrode. The $E_{1/2}$ values were determined as $1/2(E_p^a + E_p^c)$, where E_p^a and E_p^c are the anodic and cathodic peak potentials, respectively. All potentials reported are not corrected for the junction potential. The solvent in all experiments was CH_2Cl_2/CH_3CN, and the supporting electrolyte was 0.1 M tetrabutylammonium perchlorate. Differential scanning calorimetry (DSC) measurements were carried out using a Perkin-Elmer 7 series thermal analyzer at a heating rate of 10 °C/min. Thermal gravimetric analysis (TGA) measurements were performed on a Perkin-Elmer TGA7 thermal analyzer. Mass spectra (FAB) were recorded on a VG70-250S mass spectrometer. Elemental analyses were performed on a Perkin-Elmer 2400 CHN analyzer.

LEDs Fabrication and Measurement

Double-layer EL devices using compounds **3a**−**c** as the hole transport layer and Alq [tris(8-quinolinolato)-aluminum] as the emitting as well as the electron transport layer were fabricated. For comparison, a typical device using NPD as the hole transport layer was also prepared. All devices were prepared by vacuum deposition of 400 Å of the hole transporting layer, followed by 460 Å of Alq. An alloy of magnesium and silver (ca. 8:1, 500 Å) was deposited as the cathode, which was capped with 1000 Å of silver. I−V curve was measured on a Keithley 2000 source meter in an ambient environment. Light intensity was measured with a Newport 1835 optical meter.

Syntheses

Compounds 2-(*N*,*N*-diphenylamino)thiophene (**1a**), 2-[*N*-(3-methylphenyl)-*N*-phenylamino]thiophene (**1b**), 2-[*N*-(1-naphthyl)-*N*-phenylamino]thiophene (**1c**), and 9-(2-thienyl)-9*H*-carbazole (**1d**) were synthesized by similar procedures, and only the preparation of **1a** will be described in detail. Those data for **1b**−**d** are deposited as Supporting Information.

Compound 1a. To a flask containing a mixture of $(C_6H_5)_2NH$ (6.76 g, 40.0 mmol), sodium *tert*-butoxide (4.61 g, 48.0 mmol), and $Pd(OAc)_2$ (90 mg, 0.40 mmol) were added dry *o*-xylene (60 mL), 2-bromothiophene (3.87 mL, 40.0 mmol), and P(*t*-Bu)$_3$ (0.4 mL, 1.6 mmol, 0.81 M in *o*-xylene) sequentially. The solution mixture was slowly heated to reflux, stirred for 16 h, and then cooled, and 2 mL of water was added. The solution was pumped dry, and the residue was extracted with dichloromethane/water. The organic layer was dried over magnesium sulfate, filtered, and dried. The residue was chromatographed through silica gel using hexane as the eluent to give the pure 2-(*N*,*N*-diphenylamino)thiophene (**1a**) as a pale yellow crystal (6.53 g, 65%). The compound was spectroscopically identical with bona fide **1a**.[11]

Compounds 5-(*N*,*N*-diphenylamino)-2-(tri-*n*-butylstannyl)thiophene (**2a**), 5-[*N*-(3-methylphenyl)-*N*-phenylamino]-2-(tri-*n*-butylstannyl)thiophene (**2b**), 2-[*N*-(1-naphthyl)-*N*-phenylamino]-2-(tri-*n*-butylstannyl)thiophene (**2c**), and 9-[5-(1,1,1-tributylstannyl)-2-thienyl]-9*H*-carbazole (**2d**) were synthesized by similar procedures, and only the preparation of **2a** will be described in detail. Those data for **2b**−**d** are deposited as Supporting Information.

Compound 2a. A solution of *n*-BuLi (15.0 mL, 24 mmol, 1.6 M in hexane) was added to a solution of **1a** (5.03 g, 20 mmol) in 100 mL of THF at −78 °C. The solution was stirred for 30 min, then slowly warmed to room temperature over 30 min, and stirred for another 30 min. The mixture was cooled to −30 °C, and 5.42 mL (20 mmol) of tri-*n*-butylchlorostannane was added. The mixture was then warmed to room temperature and stirred for 16 h. The mixture was quenched with water (2 mL) and extracted with diethyl ether/brine. The organic layer was dried over magnesium sulfate and filtered. The solvent was removed to give a yellow oily 5-(*N*,*N*-diphenylamino)-2-(tri-*n*-butylstannyl)thiophene (**2a**) in quantitative yield. The compound **2a** was spectroscopically identical with bona fide **2a**[11] and was found to be of 95% purity. The compound was used without further purification.

Compounds tris{4-[5-(*N*,*N*-diphenylamino)-2-thienyl]-phenyl}amine (**3a**), tris{4-[5-[*N*-phenyl-*N*-(*m*-tolyl)amino]-2-thienyl]phenyl}amine (**3b**), tris{4-[5-[*N*-(1-naphthyl)-*N*-phenylamino]-2-thienyl]phenyl}amine (**3c**), and tris[4-(9-carbazolyl-2-thienyl)phenyl]amine (**3d**) were synthesized by similar procedures, and only the preparation of **3a** will be described in detail. Those data for **3b**−**d** are deposited as Supporting Information.

Compound 3a. To a flask containing a mixture of **2a** (0.99 g, 1.65 mmol, 90% purity), 4,4′,4″-tris(*p*-bromophenyl)amine (0.241 g, 0.50 mmol), and $PdCl_2(PPh_3)_2$ (21 mg, 0.030 mmol) was added 4 mL of dry dimethylformamide (DMF). The solution was slowly warmed to 80 °C and stirred for 1 h. The mixture was stirred for an additional 16 h at 60 °C. After cooling, methanol (5 mL) was added to precipitate the product. The solid was filtered, washed with methanol (2 × 5 mL), and then chromatographed with silica gel (dichloromethane/hexane = 1:4) to give a yellow powdery **3a** (0.32 g, 64%). ^{1}H NMR (acetone-d_6): δ 7.53 (d, 6 H, J = 8.4 Hz, C_6H_4), 7.31 (dd, 12 H, J = 8.4, 7.3 Hz, *m*-*H* of C_6H_5), 7.21 (s, br, 3 H, SCC*H*), 7.13 (dd, 12 H, J = 8.4, 1.3 Hz, *o*-*H* of C_6H_5), 7.09 (d, 12 H, J = 8.4 Hz, C_6H_4), 7.06 (tt, 6 H, J = 7.3, 1.3 Hz, *p*-*H* of C_6H_5), 6.69 (s, br, 3 H, SCC*H*), 2.26 (s, 3 H, C*H*$_3$). FABMS: *m*/*e* 993 (M^+). Anal. Calcd for $C_{66}H_{48}N_4S_3$: C, 79.80; H, 4.87; N, 5.64; Found: C, 79.55; H, 5.00; N, 5.88.

Compound 3b. Yield: 52%. Yellow powder. ^{1}H NMR (acetone-d_6): δ 7.53 (d, 6 H, J = 8.6 Hz, C_6H_4), 7.30 (dd, 12 H, J = 8.4, 7.3 Hz, *m*-*H* of C_6H_5), 7.22 (d, 3 H, J = 3.7 Hz, SCC*H*), 7.19 (dd, 3 H, J = 7.8, 7.4 Hz, ^{5}*H* of C_6H_4Me), 7.12 (dd, 6 H, J = 8.4, 1.2 Hz, *o*-*H* of C_6H_5),

(10) Jones, G., II; William, W. R.; Jackson, R.; Choi, C. Y.; Bergmark, W. R. *J. Phys. Chem.* **1985**, *89*, 294.

(11) Bedworth, P. V.; Cai, Y.; Jen, A.; Marder, S. R. *J. Org. Chem.* **1996**, *61*, 2242.

Table 1. Physical Data for 3a−c, TPD, NPD, and Alq

compd	T_g/T_m,[a] °C	T_d,[b] °C	λ_{max},[c] nm	E_{ox} (ΔE_p),[d] mV	HOMO/LUMO, eV
3a	107/NA	421	297, 396	111 (56), 202 (63), 383 (53), 496(73)	5.2/2.4
3b	92/NA[a]	390	297, 397	97 (50), 194 (55), 366 (58), 494 (74)	5.2/2.4
3c	127/NA[a]	412	295 sh, 397	104 (57), 204 (95), 417 (77), 502 (93)	5.2/2.4
3d	155/325	460	380	402 (62), 560 (60)	5.5/2.5
TPD	60/175	382	311, 353	314 (68)	5.4/2.3
NPD	100/265[a]	479	271, 342	342 (66)	5.4/2.3
Alq	175				5.8/3.1

[a] Obtained from DSC measurements. NA: T_m not detected. [b] Obtained from TGA measurements. [c] Measured in a CH_2Cl_2 solution. [d] Measured in CH_2Cl_2/CH_3CN (1:1). All E_{ox} data are reported relative to ferrocene which has an E_{ox} at 223 mV relative to Ag/Ag^+, and the anodic peak−cathodic peak separation (ΔE_p) is 75 mV. The concentration of the complexes used in this experiment was 5×10^{-4} M, and the scan rate was 80 mV s^{-1}.

7.09 (d, 6 H, J = 8.4 Hz, C_6H_4), 7.04 (tt, 3 H, J = 7.3 Hz, 1.2 Hz, *p-H* of C_6H_5), 6.99 (s, 3 H, ^2H of C_6H_4Me), 6.93 (d, 3 H, J = 7.8 Hz, ^4H of C_6H_4Me), 6.89 (d, 3 H, J = 7.4 Hz, ^6H of C_6H_4Me), 6.67 (d, 3 H, J = 3.7 Hz, SCC*H*), 2.26 (s, 9 H, CH_3). FABMS: *m/e* 1035 (M^+). Anal. Calcd for $C_{69}H_{54}N_4S_3$: C, 80.04; H, 5.26, N, 5.41. Found: C, 80.29; H, 5.56; N, 5.46.

Compound 3c. Yield: 68%. Golden yellow powder. ^{1}H NMR (acetone-d_6): δ 8.03 (dd, 3 H, J = 8.2, 0.8 Hz, naph), 7.99 (d, 3 H, J = 7.5 Hz, naph), 7.92 (d, 3 H, J = 8.1 Hz, naph), 7.59 (dd, 3 H, J = 7.5, 7.5 Hz, naph), 7.54−7.45 (m, 9 H, naph), 7.47 (d, 6 H, J = 8.6 Hz, C_6H_4), 7.21 (dd, 6 H, J = 8.7, 7.3 Hz, *m-H* of C_6H_5), 7.16 (d, 3 H, J = 3.8 Hz, SCC*H*), 7.04 (d, 6 H, J = 8.6 Hz, C_6H_4), 6.94 (dd, 6 H, J = 8.7, 1.1 Hz, *o-H* of C_6H_5), 7.09 (d, 6 H, J = 8.4 Hz, C_6H_4), 6.91 (tt, 3 H, J = 7.3, 1.1 Hz, *p-H* of C_6H_5), 6.67 (d, 3 H, J = 3.8 Hz, SCC*H*). FABMS: *m/e* 1145 (M^+). Anal. Calcd for $C_{78}H_{54}N_4S_3$: C, 81.93; H, 4.76; N, 4.90. Found: C, 82.06; H, 4.80; N, 4.70.

Compound 3d. Yield: 68%. Yellow powder. ^{1}H NMR ($CDCl_3$): δ 8.09 (d, 6 H, J = 7.7 Hz, carbazole), 7.56 (d, 6 H, J = 8.5 Hz, C_6H_4), 7.52 (d, 6 H, J = 8.3 Hz, carbazole), 7.43 (dd, 6 H, J = 8.3, 7.0 Hz, carbazole), 7.31 (d, 3 H, J = 3.7 Hz, SCC*H*), 7.30 (dd, 6 H, J = 7.7, 7.0 Hz, carbazole), 7.19 (d, 6 H, J = 8.5 Hz, C_6H_4), 7.15 (d, 3 H, J = 3.7 Hz, SCC*H*). FABMS: *m/e* 987 (M^+). Anal. Calcd for $C_{66}H_{42}N_4S_3$: C, 80.29; H, 4.29; N, 5.67. Found: C, 79.86; H, 4.30; N, 5.64.

Results and Discussion

Scheme 1 illustrates synthetic procedures of these new compounds. Yamamoto coupling[12] of bromothiophene with diarylamine afforded diarylthienylamine (**1a**−**d**), which was then converted to thienylstannane (**2a**−**d**). It is worth noting that a better yield of **1a**−**d** was obtained from Yamamoto coupling than from Ullmann coupling.[11] Triple thienylation of 4,4′,4″-tris(*p*-bromophenyl)amine with **2a**−**d**, using Stille's cross-coupling reaction, yielded the air-stable starburst compounds **3a**−**d**.

Compounds **3a**−**c** are amorphous and have higher glass transition temperatures (Table 1) than α-NPD (T_g = 100 °C) and TPD (T_g = 60 °C), which are commonly used as hole transport materials in organic light-emitting devices.[8] They also have very high thermal decomposition temperatures (T_d = 390−421 °C). Compound **3d** has an even higher decomposition temperature than **3a**−**c**, yet it exhibits an even higher T_g only when the melt is rapidly cooled. Crystallization and melting of the sample occurs at 212 and 325 °C, respectively, after it is heated above the glass transition temperature (Figure 1).

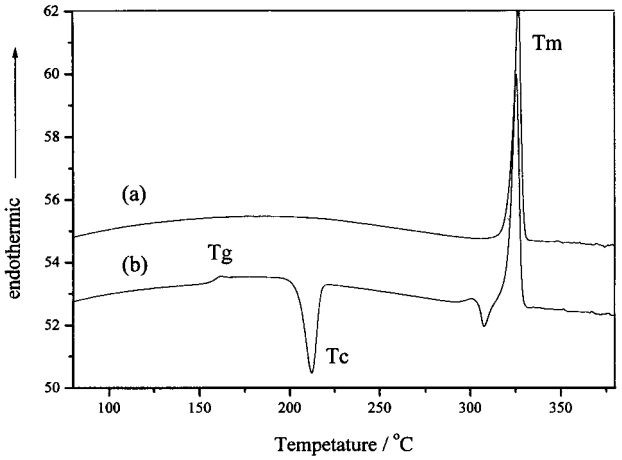

Figure 1. DSC curves for **3d** at the scan rates of 10 °C/min. (a) The first run shows only crystalline behavior with a melting transition (T_m) at 155 °C. (b) Upon rapid cooling and reheating, the second run displays a glass transition (T_g) at 155 °C, a crystallization transition (T_c) at 212 °C, and a melting transition (T_m) at 325 °C.

Scheme 1

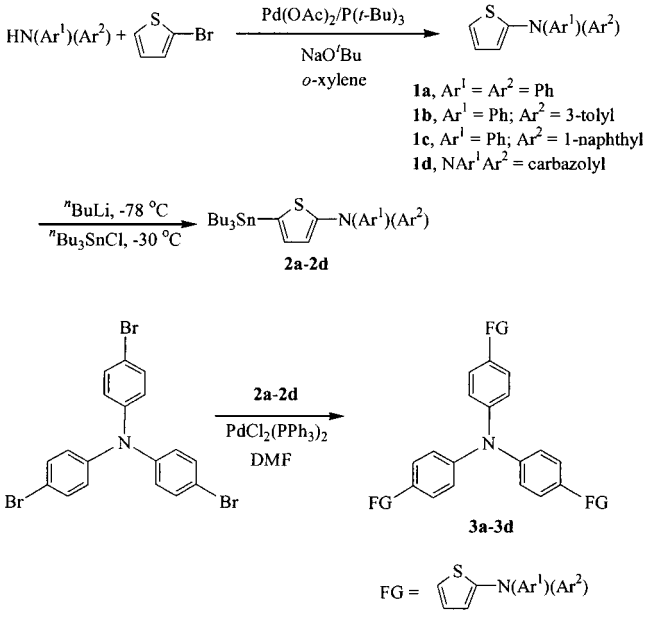

An interesting feature of the cyclic voltammetry and Osteryoung square waver voltammetry of **3a**−**c** is the observation of four successive reversible one-electron

(12) Yamamoto, T.; Nishiyama, M.; Koie, Y. *Tetrahedron Lett.* **1998**, *39*, 2367.

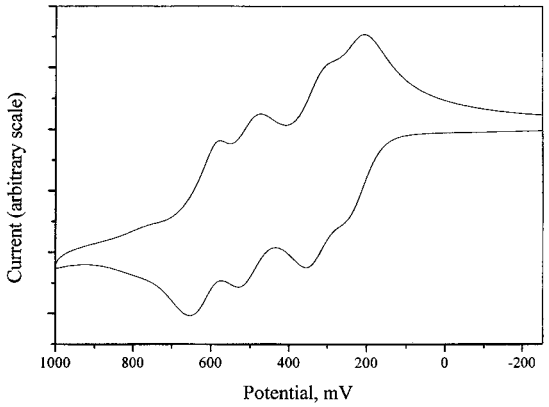

Figure 2. Cyclic voltammogram of **3a** in deoxygenated CH_2Cl_2/CH_3CN (1:1) containing 0.1 M TBAP at 25 °C. All potentials are in volts versus $Ag/AgNO_3$ (0.01 M in MeCN; scan rate is 80 mV s^{-1}).

redox processes (Figure 2). Such an outcome is attributed to the delocalization of the electron density through the entire molecule. Removal of the electron from the carbazolyl nitrogen atom appears to be much more difficult, and only the first two one-electron reversible oxidation waves can be observed for **3d**, indicating that the carbazole moiety is less electron donating than the diphenylamine moiety.[6] On the contrary, hexakis[(diarylamino)thienyl]benzene exhibits a six-electron redox process because the interaction among six amines is negligible.[6] As expected, the incorporation of an electron-rich thienyl ring[7] to the nitrogen atom results in a lower oxidation potential for **3a**−**c** compared to TPD ($\Delta E_{ox} = -214$ mV) and α-NPD ($\Delta E_{ox} = -234$ mV). The first oxidation potential of **3a**−**c** is significantly lower than the corresponding oxidation potential of hexakis[(diarylamino)thienyl]benzene[6] ($\Delta E_{ox} < -50$ mV) and further substantiates the importance of the electron resonance effect in **3a**−**c**. These electrochemical data together with the absorption spectra were used to obtain the highest occupied molecular orbital (HOMO) and lowest unoccupied molecular orbital (LUMO) energy levels of the compounds (Table 1). The HOMO energy levels of **3a**−**d** were calculated from cyclic voltammetry and by comparison with NPD (5.4 eV).[13] The LUMO/HOMO energy gap estimated from the absorption spectra were then used to obtain the LUMO energy levels.[8b,14] Those of Alq were also listed in Table 1.[13]

Double-layer EL devices using compounds **3a**−**d** as the hole transport layer and Alq as the emitting as well as electron transport layer were fabricated: I (**3a**/Alq); II (**3b**/Alq); III (**3c**/Alq); IV (**3d**/Alq). For comparison, a typical device V using NPD as the hole transport layer was also prepared. The *I*−*V*−*L* characteristics for the devices I−IV are shown in Figures 3 and 4. At $J = 100$ mA/cm^2, the driving voltages were found to be 7.83, 7.83, 9.49, 7.40, and 8.34 V, respectively, for the devices I−V. Therefore, no close relationship between the HOMO/

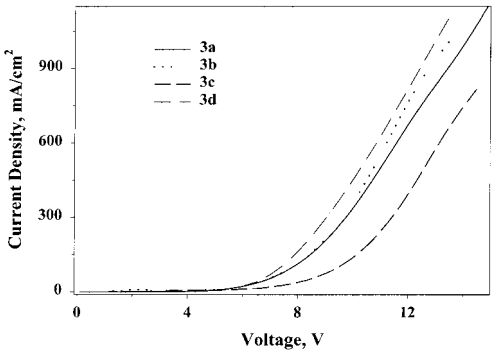

Figure 3. Current density−voltage characteristics of ITO/**3**/Alq/Mg:Ag devices.

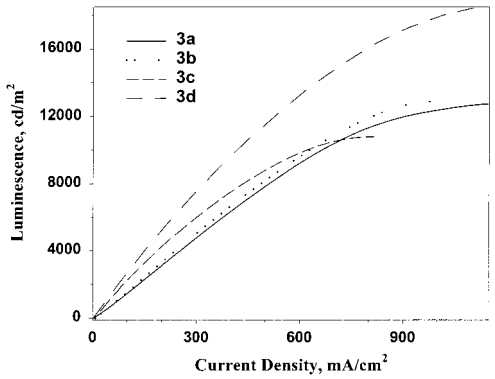

Figure 4. Luminescence−current density characteristics of ITO/**3**/Alq/Mg:Ag devices.

LUMO energy levels and the driving voltages could be established. As suggested by Adachi et al.,[15] the driving voltages may involve delicate hole/electron carrier transport and injection characteristics of the device materials. We also found the absence of a relationship between the HOMO energy and turn-on voltage, in accordance with Forrest's observations.[8a] The selection of the hole transport materials clearly affects the luminescence of the devices. The maximum luminescence (Table 2) is significantly greater as the energy barrier of the HOMO between HTL and Alq decreases. As such, the maximum luminescence of the devices IV (18661 cd/m^2) or V (25 000 cd/m^2) exceeds those of I−III considerably. Similarly, the external quantum efficiencies of the devices IV (1.1%) and V (1.2%) are higher than those of I (0.44%) and II (0.48%) at $J = 100$ mA/cm^2. Such an outcome may be attributed to the better balance of electrons and holes in the Alq layer because of more facile injection of the holes into the Alq layer in IV and V, which results in a better balance of the electrons and holes in the same layer. It is somewhat unexpected that the external quantum efficiency of the device III is 2 times those of I or II despite the similar HOMO/LUMO energy levels among the three hole transport materials. In the devices I, II, and IV, green light emission from Alq at 529 nm was observed (Figure 5). The EL spectra of I, II, and IV are almost superimposable. However, they are red-shifted to that of the device V by 18 nm. Furthermore, the half-width of the half-intensity (hwhi ∼ 90 nm) of their EL spectra is slightly greater than that of V (hwhi ∼ 86 nm). These phenomena may

(13) (a) Baldo, M. A.; Thompson, M. E.; Forrest, S. R. *Pure Appl. Chem.* **1999**, *71*, 2095. (b) O'Brien, D. F.; Baldo, M. A.; Thompson, M. E.; Forrest, S. R. *Appl. Phys. Lett.* **1999**, *74*, 442. (c) Kwong, R. C.; Lamansky, S.; Thompson, M. E. *Adv. Mater.* **2000**, *12*, 1134. (d) Baldo, M. A.; Thompson, M. E.; Forrest, S. R. *Nature* **2000**, *403*, 750.

(14) (a) Thelakkat, M.; Schmidt, H.-W. *Adv. Mater.* **1998**, *10*, 219. (b) Janietz, S.; Bradley, D. D. C.; Grell, M.; Giebeler, C.; Inbasekaran, M.; Woo, E. P. *Appl. Phys. Lett.* **1998**, *73*, 2453.

(15) Tamoto, N.; Adachi, C.; Nagai, K. *Chem. Mater.* **1997**, *9*, 1077.

Table 2. Performance Characteristics of the Devices

device	turn-on voltage, V	max brightness, cd/m^2	max ext. quant. efficiency, %	voltage,[a] V	brightness,[a] cd/m^2	ext. quant. efficiency,[a] %	power efficiency,[a] lm/W
I[b]	3.7	12 728 at 14.9 V	0.48 at 10.1 V	7.8	1453	0.44	0.59
II[c]	3.8	12 888 at 13.5 V	0.52 at 9.8 V	7.8	1548	0.48	0.62
III[d]	4.0	10 793 at 14.5 V	0.96 at 9.2 V	9.5	2240	0.95	0.74
IV[e]	3.7	18 661 at 14 V	1.1 at 7.5 V	7.4	2689	1.1	1.1
V[f]	4.5	25 000 at 15 V	1.3 at 8.2 V	8.3	3629	1.2	1.2
VI[g]	4.5	3 500 at 13.5 V	0.81 at 7.5 V	8.2	986	0.76	0.36

[a] $\times$100 mA/cm^2. [b] ITO/**3a** (400 Å)/Alq (400 Å)/Mg:Ag. [c] ITO/**3b** (400 Å)/Alq (400 Å)/Mg:Ag. [d] ITO/**3c** (400 Å)/Alq (400 Å)/Mg:Ag. [e] ITO/**3d** (365 Å)/Alq (350 Å)/Mg:Ag. [f] ITO/NPD (400 Å)/Alq (400 Å)/Mg:Ag. [g] ITO/**3d** (365 Å)/BCP (120 Å)/Alq (150 Å)/Mg:Ag.

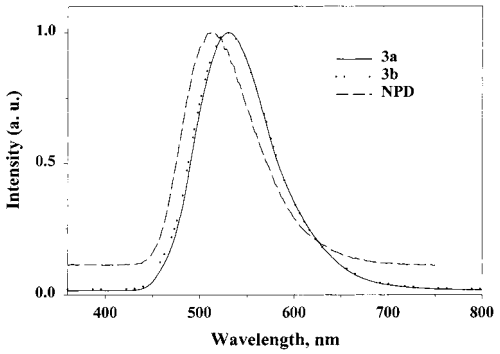

Figure 5. EL spectra of the devices I (**3a**/Alq), II (**3b**/Alq), and V (NPD/Alq).

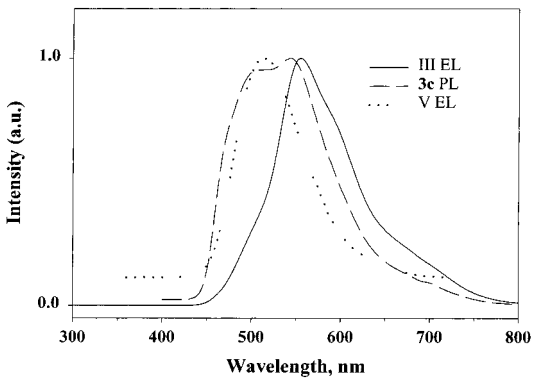

Figure 6. EL spectra of the devices III (**3c**/Alq) and V (NPD/Alq) and a PL spectrum of a film of **3c**.

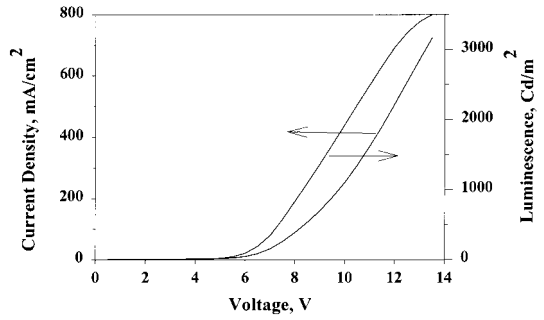

Figure 7. Current density−voltage and luminescence−current density characteristics of a ITO/**3d**/BCP/Alq/Mg:Ag device.

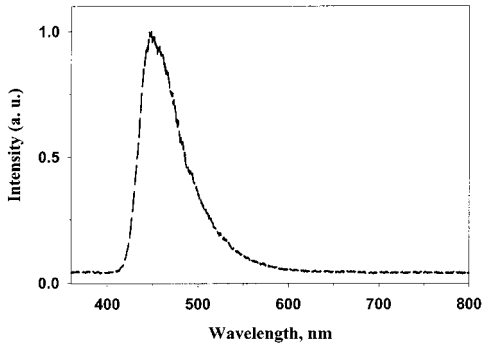

Figure 8. EL spectrum of a ITO/**3d**/BCP/Alq/Mg:Ag device.

be attributed to the exciplex formation, in accordance with Adachi's finding through careful studies on a series of double-layer (HTL/EL) devices.[15] Formation of exciplexes between Alq and arylamines is not a rare example, particularly when the amines have a low ionization potential.[15,16] The EL spectrum of the device III is different from those of the devices I, II, and IV. In this device, the emitted green light was mixed with some red light at ~680 nm (Figure 6). Contribution of emission from **3c** alone is minimal if any in view of the dissimilarity between the EL spectrum of the device III and the photoluminescence (PL) spectrum of the film **3c** (Figure 6) and the rather weak intensity of the latter. Contribution from the charge-transfer complex to 680 nm emission can be eliminated because the absorption spectra of the mixed films of **3c** and Alq show only superposition of each absorption spectrum. The increment of hwhi (100 nm) as well as the red shift of the EL spectrum of III (λ_{em} = 554 nm) relative to that of V (λ_{em} = 512 nm) suggests that exciplex also forms in the device III. The presence of an electroplex may also be possible in view of the shoulder at ~500 nm.[17]

Although **3d** emits blue light with good quantum efficiency in the solution (Φ = 0.4 in CH_2Cl_2; λ_{em} = 444 nm; λ_{abs} = 380 nm), only EL spectra characteristic of Alq were detected in the device IV (ITO/**3d**/Alq/Mg:Ag), indicating no exciton formation in the layer of **3d**. To confine the exciton inside the layer of **3d**, a layer of 2,9-dimethyl-4,7-diphenyl-1,10-phenanthroline (bathocuproine, abbreviated as BCP),[13] which has HOMO and LUMO levels at 6.4 and 2.9 eV, respectively, was inserted between **3d** and Alq. It is anticipated that electrons can move freely from Alq through BCP to **3d**, whereas BCP effectively blocks the passage of holes out of the **3d** layer because of the large energy barrier. Indeed, light was emitted solely from the layer of **3d** in the device VI (ITO/**3d**/BCP/Alq/Mg:Ag) with a maximum luminescence at 3500 cd/m^2 (Figure 7) and an emission wavelength at 448 nm (Figure 8).

In summary, we have synthesized new star-shaped molecules which possess high T_g and thermal stability; they can be used as hole transport and/or blue-light-

(16) Itano, K.; Ogawa, H.; Shirota, Y. *Appl. Phys. Lett.* **1998**, *72*, 636.

(17) (a) Giro, G.; Cocchi, M.; Kalinowski, J.; Di Marco, P.; Fattori, V. *Chem. Phys. Lett.* **2000**, *318*, 137. (b) Kalinowski, J.; Giro, G.; Cocchi, M.; Fattori, V.; Di Marco, P. *Appl. Phys. Lett.* **2000**, *76*, 2352.

emitting materials in EL devices. Variation of the film thickness as well as the devices consisting of double hole transport layers[9] is currently ongoing to optimize the performance of the devices fabricated from **3a**−**d**. Our preliminary results indicate that the synthetic strategy used in this can be extended to dendritic molecules. The results will be reported in due course.

Acknowledgment. This work was supported by Academia Sinica and Chinese Petroleum Co.

Supporting Information Available: Data are presented for compounds **1b**−**d**, **2b**−**d**, and **3b**−**d** (PDF). This material is available free of charge via the Internet at http://pubs.acs.org.

CM0100568